



Electrochemical, Gravimetric and Thermodynamic studies of corrosion inhibitive performance of *Treculiaafricana* on AA7075-T7351 in 1.0 M HCl

S. C. Udensi^{1,2*}, O. E. Ekpe¹, L. A. Nnanna¹

¹Department of Physics, Michael Okpara University of Agriculture Umudike, P.M.B 7267, Umudike, Abia State, Nigeria.

² Department of Physics, Federal University of Technology Owerri, P.M.B 1526, Owerri, Imo State, Nigeria

Received 22 Oct2019,
Revised 01 Nov 2019,
Accepted 03 Nov 2019

Keywords

- ✓ *Treculiaafricana*,
- ✓ Electrochemical,
- ✓ Green inhibitor,
- ✓ Gravimetric,
- ✓ Adsorption,
- ✓ AA7075.

solomon.udensi@futo.edu.ng

Phone: +2348160803777

Abstract

The inhibiting effects of flavonoid-, kavaflavone-, and phenolic-rich *Treculia africana*(TA) leaves extracts on the corrosion of AA7075-T7351 in 1.0 M HCl have been investigated using gravimetric, electrochemical and thermodynamic techniques. Gravimetric studies showed that increase in TA concentration in the acidic environment, enhanced the inhibition efficiency of TA extract, but reduced with increase in temperature. The inhibiting property of TA was achieved through an endothermic physisorption and chemisorption of a protective layer of TA on AA7075-T7351 which fitted well to Langmuir, Freundlich and Temkin adsorption isotherms, in the order Langmuir > Freundlich > Temkin. TA molecules were found to belong to the class of mixed-type corrosion inhibitors, with more dominant cathodic property. Potentiodynamic polarization (PDP) and electrochemical impedance spectroscopy (EIS) results further supported the mixed-type character of TA through the existence of an AA7075-T7351/acid interface which reduced current flow with increase in concentration. High values of adsorption coefficient, K_{ads} , obtained from Temkin isotherms showed strong and spontaneous adsorption of TA on the AA7075-T7351.

1. Introduction

Aluminium alloys and their composites are materials of choice, for structural and mechanical fabrications, because of the ease of engineering them to produce materials with better and improved wear resistance, tensile property, fracture toughness, fatigue life, etc. [1, 2]. Hence, they are used in fabricating the fuselage, wings, and engine baffles of airplanes, in military hardware, in marine and automotive industries [3], even in food industries for packaging because of their competitive corrosion resistant property [4]. AA7075-T7351 is one of such aluminium alloys used in the aforementioned applications, because of its high fracture toughness, better stress corrosion resistance (than AA7075-T6), good strength - to - weight ratio and high zinc content (about 5.8% for our samples). One drawback of using AA7075-T7351 as engineering material is the precipitation of MgZn₂ particles at the grain boundaries, susceptible to corrosion at elevated temperatures [5].

The premature termination of the valuable function of any metal is the key factor that failure by corrosion has occurred, as a result of the interaction of the metal with its environment [6]. These failures vary according to service conditions and include: corrosion product contamination of sensitive materials, like paints and food; corrosion product interference with heat transfer; loss of aesthetic appeal, failure by environmentally sensitive cracking; perforation by pitting corrosion causing leaks in tanks and pipes etc. [7, 8].

Hitherto, corrosion inhibitions of AA7075-T7351 are carried out by the addition of inorganic cationic substances like Ce³⁺, La³⁺, Pr³⁺, Nd³⁺ and Ni³⁺[9], chromates[10], silicates, tungstates etc. [11] to the corrodents. However, because of the toxic nature of these inorganic substances and their consequent deleterious effects on our flora and fauna, stringent laws have been promulgated to discontinue their usage, in order to guard against food and body implant contaminations [4, 12]; protect marine life and the entire ecosystem, as well as encourage production of novel, toxin-free materials for engineering construction [13, 14].

Recently, a flurry of activities has been on-going in the use of native flora [15, 16], which offer environmentally friendly corrosion inhibitive alternative. The advantage being that these plants had either been used as food or herb for centuries. Luckily, it has been reported by many researchers that, in acidic or alkaline environments, certain naturally occurring and synthetic aromatic substances containing heteroatoms, like, nitrogen, phosphorous, oxygen and /or sulphur [17, 18, 19] and consisting of double and triple bonds are some of the most convenient and economical ways of managing metal corrosion.

Aluminium readily forms a stable protective layer of amphoteric aluminium oxide when exposed to the elements, which impedes further degradation of the parent alloy. However, when these amphoteric films on the parent aluminium alloys come in contact with harsher alkaline or acidic environments, they corrode through chemical [20], electrochemical [21], and/or biological processes [22].

Corrosion inhibition in acidic medium as reported by Sharma and Sharma [15], used *Psidium Guajava* seeds extract in HCl solution to analyze the corrosion properties of aluminum. Their study showed increased corrosion inhibition of aluminum with increased extract concentration but a reduction in inhibition efficiency with increase in temperature. Elsewhere, other researchers who used organic extracts in acidic solutions for studying the corrosion behaviour of aluminium, with equally successful results include: the use of dry arecanut seed extract in 0.5 M HCl by Raghavendra and Bhat [23]; *Trigonellafoenum-graecum L* seed extracts in 1 M HCl by Ennouri and co-workers [24]; Lupine extract in 0.1 M HCl, 0.1 M HClO₄ and 0.05 M H₂SO₄ by Abd-El-Naby and coworkers [25] etc.

Also in alkaline environments, studies on aluminium corrosion behaviours were equally rewarding in their inhibition efficiencies. For instance Nnanna and coworkers used *Palisota hirsute* extract in 0.25 M KOH [16]. Other extracts used in alkaline environments include: *Sansevieratrifasciata* extract in 2M KOH [26]; *Piper longum* extract and Kalmegh leaf extract in 1 M NaOH [27]; peel extracts from *Pisum sativum*, *Solanum tuberosum* and *Citrus reticulata* in 1 M NaOH solution [28]; *Apium graveolens L.* seed extract in 0.25 M NaOH solution [29] etc.

In this present work, the inhibitive behaviour of freshly prepared *Treculia africana* leaf extracts on AA7075-T7351 in 1.0 M HCl has been studied and reported. The phytochemical study of *Treculia africana* reveal high content of phenols, terpenes, flavonoids, tannins, etc. [30, 31]

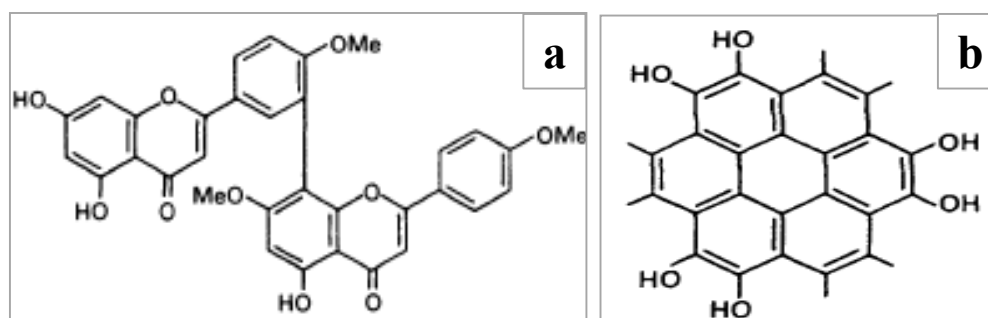


Figure 1: Flavonoid molecular structure of a woody plant, kayaflavone (a) and phenolic polymer partial molecular structure of leaves, plant melanin (b).

2. Material and Methods

2.1. Materials preparation

The AA7075-T7351 specimens used in this study were obtained from Kaiser aluminium, USA, with order no 43133135-1, in the form of sawn plates (365.03 cm x 123.19cm x 0.635 cm). The elemental compositions of the aluminium alloy is as follows (wt %); Al = 89.53, Zn = 5.80, Mg = 2.50, Cu = 1.60, Cr = 0.20, Fe = 0.16, Si = 0.07, Ti = 0.03, Mn = 0.03, Zr = 0.02, V = 0.01, others = 0.05). The aluminium alloy plates were sawn into 2 cm x 2 cm x 0.635 cm coupons, and a hole drilled near the top of each coupon, through which a plastic thread would be attached, in order to aid dipping into the corrosive environments during the gravimetric measurement. Subsequently the coupons were polished using emery cloth of varying fineness (240 and 320 grits), also the edges were abraded in order to remove burrs. Then, they were copiously washed with distilled water, degreased in acetone and hot air dried according to ASTM G1 - 03 (2003) specification [32].

Treculia africana (TA) leaves were procured from the farm area of Umuegwu Okpuala, Afugiri, Umuahia, Abia State, Nigeria, washed in copious amount of water, air dried under room temperature conditions - for thirty days - and ground to aid extraction. The extract was obtained with the aid of a severally refluxed (5 times) azeotrope mixture of ethanol and water (as solvent, i.e. 4.5% water and 95.5% ethanol), whose boiling point is 78.2 °C in asoxhlet extractor containing the ground dried leaves. The concentrated solutions containing

the extracts were then evaporated in an oven and a brownish semisolid residue obtained and kept away in a desiccator for further use. The extraction yield using the Azeotrope mixture was 1.5 % (15 g of extract per litre) for *Treculia Africana*.

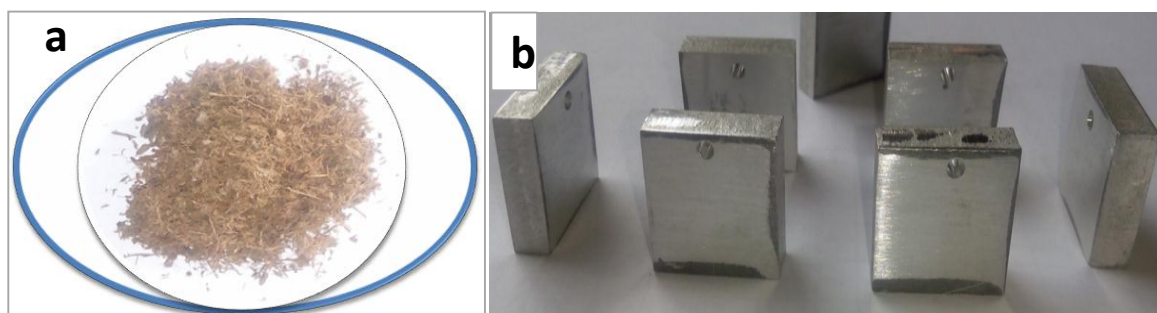


Figure 2: Ground dried *Treculiaafricana* leaves (a); the perforated AA7075-T7351 coupons used in the study (b)

Also, 1.0 M HCl used in this work was produced from 37 % HCl per litre; with density of 1.2 g/cm³; vapour pressures of 22.3 KPa (21.1 °C), 54.7 KPa (37.7 °C); vapour density of 1.3 (versus air) and a concentration of 12 M.

2.2. Gravimetric measurements

The experiments were performed under room temperature conditions (25 ± 1°C), by introducing 0.1, 0.2, 0.3, 0.4 and 0.5g of TA extracts into five different beakers containing 1.0 M HCl. Subsequently, previously 'ASTM standard' cleaned and weighed AA7075-T7351 samples were immersed in the 1.0 M HCl environments with and without TA extracts, with the aid of a plastic thread [33], after which it was allowed to run for 1, 2, 3, 4, 5, 6, and 7 hrs. The coupons were then cleaned mechanically by scrubbing them with a soft bristle brush, ultrasonicated, hot air dried and reweighed using an FA2104 digital weighing balance of 0.01 mg precision, according to ASTM G 31 - 72 (2004) standard [34]. The same procedure was repeated thrice, to certify the reliability of the outcome (which was above 98 % reproducible). The corrosion rate (CR) and inhibition efficiency (I.E.) were respectively derived using equations 1, 2 and 3 [14, 15];

$$CR = \frac{87.6\Delta W}{\rho A t} \quad (1)$$

$$\theta = 1 - \frac{CR_i}{CR_{ui}} \quad (2)$$

$$IE = 100\theta \quad (3)$$

where ΔW is the weight loss after immersion in the inhibited and uninhibited environments, ρ is the density of AA7075-T7351 slide (gcm⁻³), A is the surface area of the slide, t is the immersion/exposure time (hr), θ is the surface coverage, CR_i is the corrosion rate in the presence of NBL and CR_{ui} is the corrosion rate in the absence of NBL.

Elsewhere, the effect of temperature on the gravimetric measurements of the corrosion inhibition efficiency of TA on AA7075-T7351 in 1.0 M HCl, were performed at increased temperatures of 40, 50, 60 and 65°C. Corrosion rate is a temperature dependent quantity, which makes it convenient to use Arrhenius-like equations to represent it. These equations can be linearized thus

$$\log CR = \log A - \frac{E_a}{2.303RT} \quad (4)$$

$$\log\left(\frac{CR}{T}\right) = \left(\log\left(\frac{R}{Nh}\right) + \frac{\Delta S_a^0}{2.303R}\right) - \frac{\Delta H_a^0}{2.303RT} \quad (5)$$

where A = Arrhenius pre-exponential factor, R = gas constant (8.3145 J/(mol.K)), h = Planck's constant, N = Avogadro's number, T = absolute temperature (i.e. 273 + θ)°K, ΔS_a^0 = apparent entropy of activation (J/(mol.K)),

ΔH_a^0 = apparent enthalpy of activation (KJ/mol), E_a = apparent activation energy (i.e. minimum amount of energy required to generate corrosion products, like scales and rust) [14].

2.3. Electrochemical measurements

Electrochemical experiments to determine the corrosion characteristics of AA7075-T7351 in the presence and absence of TA were implemented in a conventional three electrode system using an AFCBP 1 bipotentiostat. The exposure area of each AA7075-T7351 working electrode (WE) in the test environment was 1 cm². While a piece of platinum wire and saturated calomel electrode were used as counter electrode (CE) and reference electrode (RE) respectively. Prior to the insertion of the WE inside the electrochemical cell, the coupons were polished with emery cloths of different fineness, washed with copious amount of distilled water and sonicated in ethanol, in line with ASTM standards [32, 34]. All measurements were carried out in triplicate, in a non deaerated, unstirred environments at room temperature conditions (25 ± 1°C).

Preceding each experiment the working electrode (AA7075-T7351) was allowed to corrode freely for 60 minutes to establish an open circuit potential (OCP) or the corrosion potential E_{corr} . Potentiodynamic polarization were made by automatically changing the potential range, from cathode to anode, ±500 mV_{SCE} relative to OCP, at a scan rate of 1 mVs⁻¹. The inhibition efficiency (I.E.) of TA in 1.0 M HCl was calculated using;

$$IE = 100 \times \left(1 - \frac{I_{corr}^i}{I_{corr}^{ui}} \right) \% \quad (6)$$

where I_{corr}^{ui} is the corrosion current density, in the uninhibited 1.0 M HCl and I_{corr}^i is the corrosion current density, in the inhibited 1.0 M HCl (i.e. presence of the leaf extract).

Electrochemical impedance spectroscopy (EIS) measurements for all samples were made in the frequency range, 100 KHz to 100 mHz, with a little alternating voltage perturbation of ±100mV at E_{corr} . The inhibition efficiency (I.E.) of TA in 1.0 M HCl was calculated using

$$IE = 100 \times \left(1 - \frac{R_{ct}^{ui}}{R_{ct}^i} \right) \% \quad (7)$$

where R_{ct}^{ui} is the charge transfer resistance, in the uninhibited 1.0 M HCl and R_{ct}^i is the charge transfer resistance, in the inhibited 1.0 M HCl (i.e. presence of the leaf extract).

3. Results and discussion

3.1. Gravimetric measurement and temperature effect

The knowledge of the effect of temperature on the corrosion rates and inhibition efficiencies of inhibitors are important because of the many changes occurring at the metal - liquid interface, for example, rearrangement and/or decomposition of the inhibitor, enhanced etching of the metal with increase in temperature etc [39]. Figures 3 (a) and (b) respectively show the plots of corrosion rate (CR) and Inhibition efficiency (I.E.) against TA concentrations for AA7075-T7351 in 1.0 M HCl environment at different temperatures. It is seen from figure 3 (a) that the CR of AA7075-T7351 at room temperature (298 ± 1 K) reduced with increase in TA concentration. This is confirmed by figure 3 (b), where an inhibition efficiency of 85.21 % was obtained for 0.6 g/L TA in 1.0 M HCl. This indicates that the surfaces of AA7075-T7351 coupons were screened from the corrosive environment due to adsorption of TA molecules on the Aluminium coupons to form an AA7075-T7351 - TA complex barrier [39].

However, with increase in the temperature (i.e. from 298 K to 313, 323, 333 and 338 K) of the corrosive environment, the CR increased, for each TA concentration. This is because the rate of oxidation of AA7075-T7351 equals the rate of reduction of hydrogen ions, which are both temperature dependent [35, 36]. Although, This also led to the rapid degradation of the complex barrier and eventual desorption of TA molecules already adhered to AA7075-T7351.

Figure 4a and 4b show the Arrhenius plot of AA7075-T7351 in 1 M HCl in the presence and absence of TA extracts, at different concentrations, from which the thermodynamic parameters, such as the energy of activation E_a^0 , the entropy of activation ΔS_a^0 and the enthalpy of activation ΔH_a^0 are shown in table 1, after 3 hours.

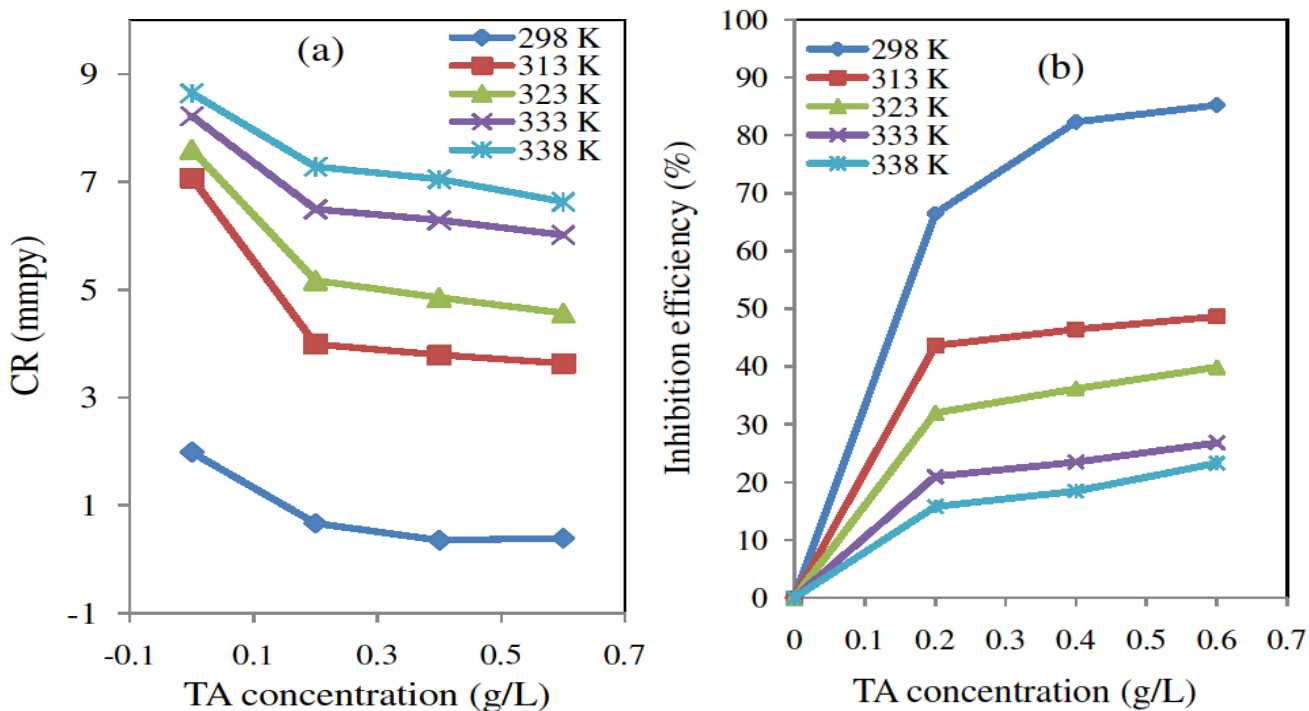


Figure 3: Variations of corrosion rate (a) and inhibition efficiency (b) with TA concentrations for AA7075-T7351 in 1.0 M HCl environment at different temperatures from the gravimetric studies.

Table 1: Calculated kinetic parameters including apparent activation energy, entropy change, enthalpy change, and Arrhenius pre- exponential factors for AA7075-T7351 in 1 M HCl in the absence and presence of *Treculia africana* after 3 hours

Time	Concentration	A	E_a (KJ/g)	ΔH_a^0 (KJ/g)	ΔS_a^0 (J/g.K)
3 hrs	Uninhibited	102.33	6.97	4.26	-215.5
	200 mg	13274	21.10	18.40	-175.1
	400 mg	17620	21.98	19.28	-172.7
	600 mg	14454	21.58	18.89	-174.4

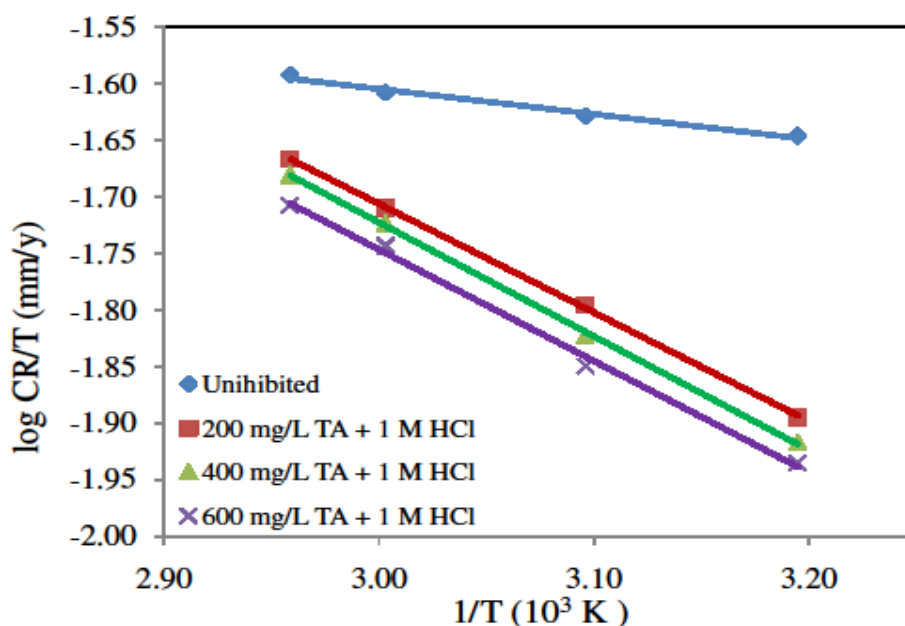


Fig.4a: Arrhenius plots for the corrosion of AA7075 in 1M HCl in the absence and presence of *Treculia africana* after 3 hrs

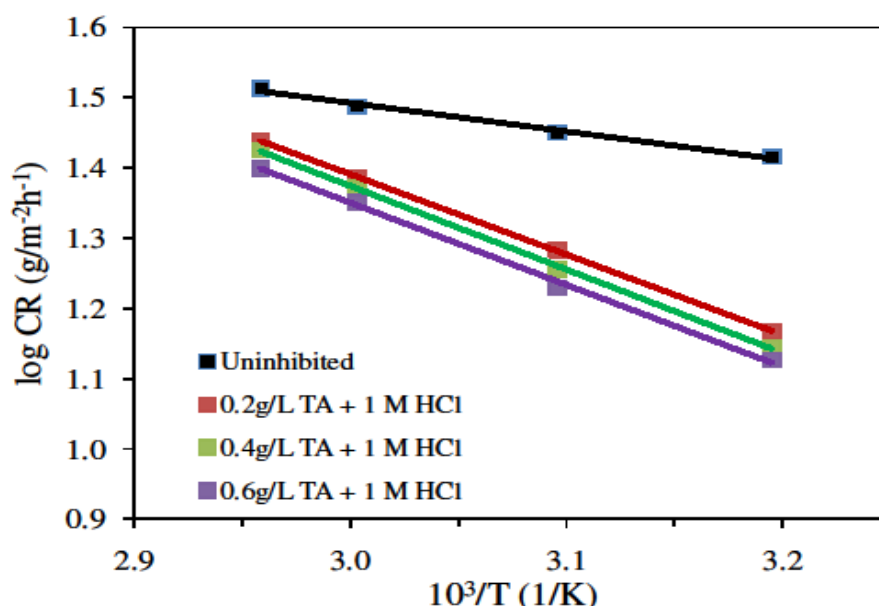


Fig. 4b: Alternative Arrhenius plots for the corrosion of AA7075 in 1M HCl in the absence and presence of *Treculia africana* after 3 hrs.

The values of the energy of activation in the presence of TA extracts are higher than the uninhibited corrosive environment. This indicates a slower reaction rate for surface coverage and explains why the inhibition efficiencies decreased with increase in temperatures [39]. ΔH_a^0 is positive showing that AA7075-T7351 dissolution in 1 M HCl is difficult and endothermic in nature [45]. Also the entropy of activation ΔS_a^0 , became less negative with increase in concentration. This indicates an ordered arrangement of TA molecules on the Aluminium surface, signifying that the activated complex is an association and not a dissociation step in the rate determining step [45].

3.2 Adsorption isotherms and results

The TA molecules achieved inhibition by the displacement of water molecules on AA7075-T7351 surface, through the following equation [37, 38];



where Inh_{sol} are the TA molecules added into the solution and Inh_{ads} are the adsorbed TA molecules on the AA7075-T7351 surface, y is the number of the initially adsorbed water molecule displaced by the inhibitor TA molecules. The mechanisms of adsorption were fitted/tested using popular adsorption isotherms namely; Langmuir, Freundlich, and Temkin, to gain insight on the type of double layer structure involved, the thermodynamics of the organo - electrochemical reaction taking place on the AA7075-T7351 surface and how these inhibitors are affected by temperatures (313, 323, 333, 338 K) [33, 37]. These three isotherms, in equation forms are represented thus;

$$\frac{\theta}{1-\theta} = C_{\text{Inh}} K_{\text{ads}} \quad \dots \text{Langmuir} \quad (9)$$

$$\log \theta = \log K_{\text{ads}} + \frac{1}{n} \log C_{\text{Inh}} \quad \dots \text{Freundlich} \quad (10)$$

$$\theta = \frac{-1}{2a} \ln K_{\text{ads}} + \frac{-1}{2a} C_{\text{Inh}} \quad \dots \text{Temkin} \quad (11)$$

where θ = surface coverage, C_{inh} = inhibitor concentration, K_{ads} = equilibrium adsorption coefficient, a = a sign dependent molecular interaction parameter and n = an exponent characteristic of the type of adsorbate.

The equilibrium adsorption coefficient is related to the standard Gibb's free energy of adsorption, ΔG_{ads}^0 , through the equation below;

$$\Delta G_{ads}^0 = -RT \ln 1000 K_{ads} \quad (12)$$

where R is the universal gas constant; 1000 g/L (or mL/L) is the molar concentration of water in bulk solution. Table 2 shows that Langmuir (figure 5) has the highest regression coefficient (R^2), followed closely by Freundlich (figure 6) and after that Temkin (figure 7). There was a decrease in K_{ads} values as temperature increased, for Langmuir and Freundlich indicating physical adsorption or electrostatic attraction of the charged hydrophilic group from the TA extract and the charged active sites on the AA7075-T7351 surface. The free energy of adsorption (ΔG_{ads}^0) values are negative, indicating spontaneous adsorption process and stability on the AA7075-T7351 surface [46]. The values of free energy of adsorption obtained for Langmuir and Freundlich are approximately 16 KJ/g, indicating good agreement with each other. The reciprocals of n obtained under Freundlich are less than 1, indicating that adsorption is easy [47].

The high values of K_{ads} obtained from Temkin 52.14 to 78.17×10^3 l/g indicate a strong and spontaneous adsorption on the AA7075-T7351 surface through chemisorption process [33, 39]. This is corroborated by the negative values of constant a, indicating a strong repulsive force between the adsorbate and adsorbent layers.

Table 2: Equilibrium adsorption parameters and regression coefficients for the adsorption of TA on AA7075-T7351 in 1.0 M HCl at different temperature obtained from Langmuir, Freundlich and Temkin adsorption isotherms

T (K)	Langmuir			Freundlich				Temkin			
	K_{ads} (l/g)	ΔG_{ads}^0 (KJ/g)	R^2	K_{ads} (l/g)	ΔG_{ads}^0 (KJ/g)	n	R^2	K_{ads} (l/g)	ΔG_{ads}^0 (KJ/g)	a	R^2
313	0.432	-15.79	0.998	0.511	-16.23	10.31	0.995	78172	-47.30	-11.111	0.993
323	0.485	-16.61	1.000	0.439	-16.34	5.025	0.992	439.00	-34.89	-7.042	0.986
333	0.251	-15.30	0.988	0.294	-15.74	4.651	0.960	289.07	-34.82	-9.804	0.945
338	0.291	-15.94	0.964	0.268	-15.71	2.933	0.932	52.14	-30.52	-7.692	0.903

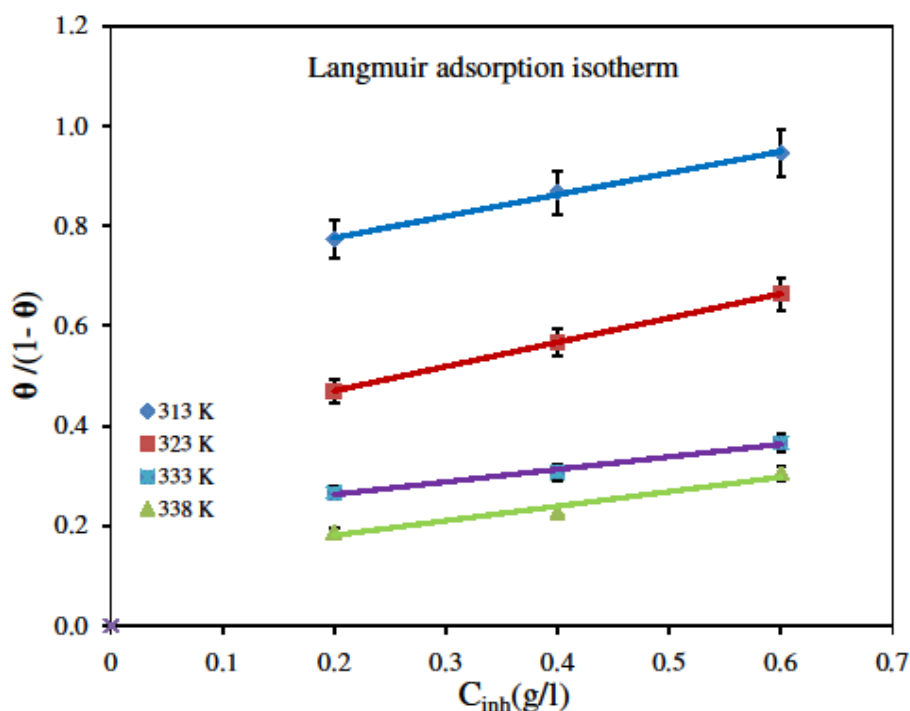


Figure 5: Langmuir adsorption isotherm plot (left) and the corresponding plot for the determination of enthalpy and entropy of TA adsorption on AA7075-T7351 surface in 1.0 M HCl

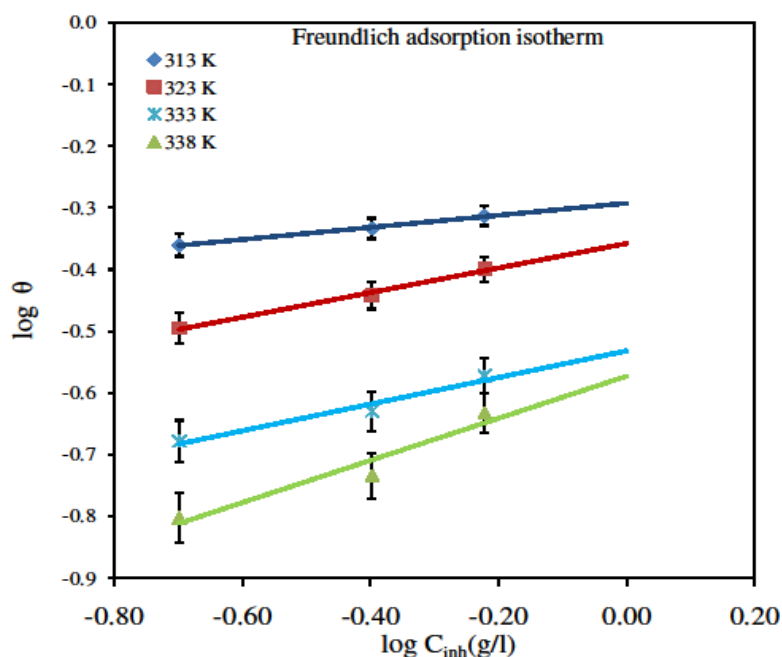


Figure 6: Freundlich adsorption isotherm plot (left) and the corresponding plot for the determination of enthalpy and entropy of TA adsorption on AA7075-T7351 surface in 1.0 M HCl

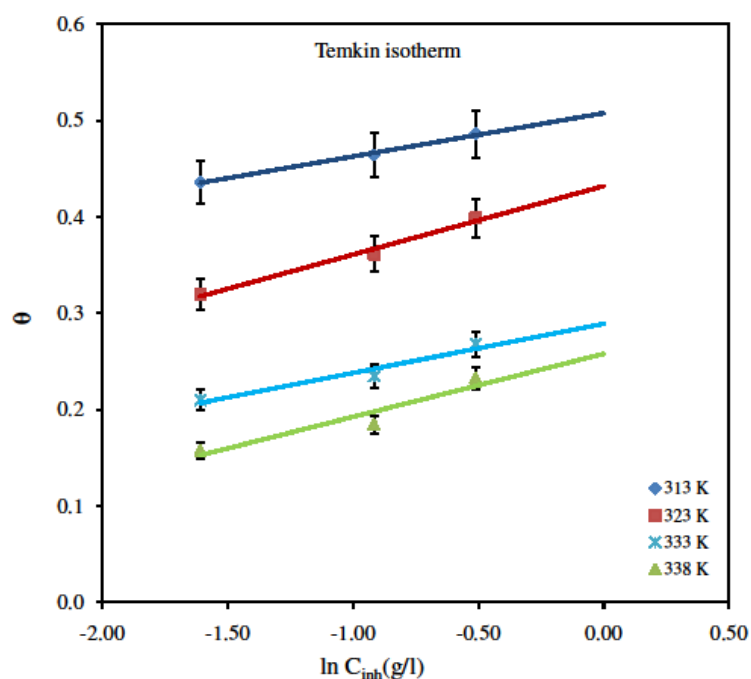


Figure 7: Temkin adsorption isotherm plot (left) and the corresponding plot for the determination of enthalpy and entropy of TA adsorption on AA7075-T7351 surface in 1.0M HCl

3.3. Electrochemical measurement results

3.3.1 Potentiodynamic Polarization

Tafel polarization plots of AA7075-T7351 in 1.0 M HCl in the presence and absence of TA inhibitors are shown in figure 8, from where the corrosion polarization parameters were derived and listed in table 3. The table shows that both the Tafel anodic slope, β_a and Tafel cathodic slope, β_c were affected by TA introduction in the acid. Indicating that TA is a mixed-type corrosion inhibitor [38, 41] and affects both oxidative, anodic reaction (i.e. AA7075-T7351 dissolution) and reductive, cathodic reaction (i.e. hydrogen evolution) [42]. The displacements' magnitudes from the open circuit potential (E_{corr}) of the uninhibited solutions are 41, 33, 21 and 11 mV for 100, 200, 500 and 1000 mg/L TA. The displacements which were to lesser overpotential suggested

that cathode-type corrosion inhibition dominated. There was a significant decrease in corrosion current density as the inhibitor concentration increased, as a result of the capacitive double layer which blocks off charge movement round the circuit (i.e. 10.08 $\mu\text{A}/\text{cm}^2$, 9.49 $\mu\text{A}/\text{cm}^2$, 5.56 $\mu\text{A}/\text{cm}^2$ and 3.99 $\mu\text{A}/\text{cm}^2$ for 100, 200, 500, and 1000 mg/L TA respectively, see table 4). This resulted in a gradual increase in inhibition efficiency that reached a maximum of 85 % at 1000 mg/L concentration of TA.

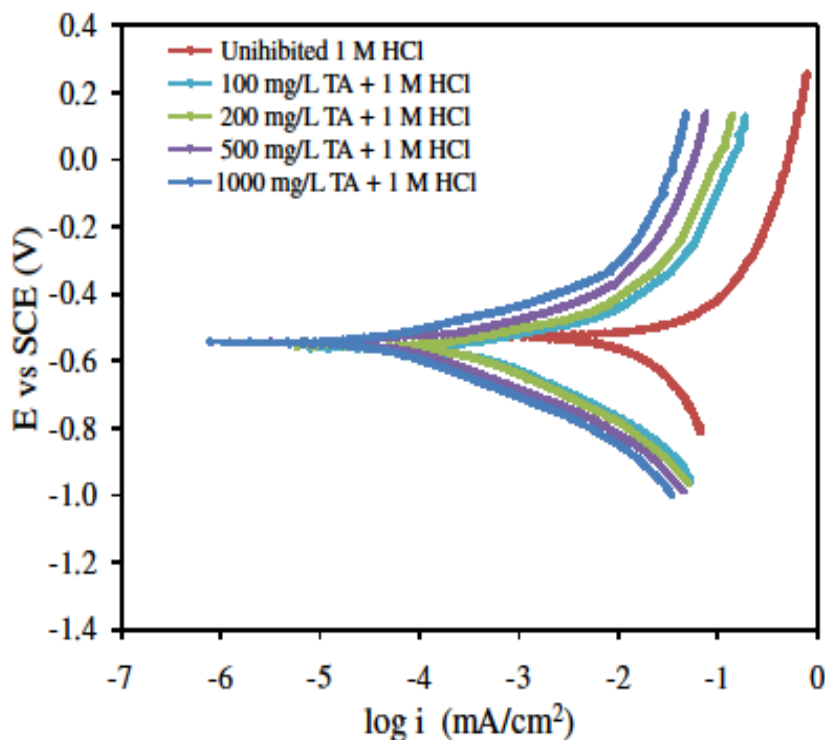


Figure 8: Potentiodynamic polarization plots for AA7075-T7351 in 1.0 M HCl in the absence and presence of TA

Table 3: Potentiodynamic polarization results for AA7075-T7351 in 1.0 M HCl in the absence and presence of TA

System (1.0 M HCl)	E_{corr} (mV vs SCE)	I_{corr} ($\mu\text{A}/\text{cm}^2$)	β_a (V/dec)	β_c (V/dec)	IE(%)	θ
Uninhibited	-526	26.67	0.159	0.695		
100 mg/L TA	-567	10.08	0.369	0.482	62.2	0.622
200 mg/L TA	-559	9.49	0.433	0.499	64.4	0.644
500 mg/L TA	-547	5.56	0.434	0.460	79.2	0.792
1000 mg/L TA	-537	3.99	0.442	0.468	85.0	0.850

3.3.2 Electrochemical Impedance Spectroscopy (EIS)

The kinetics and character of the electrochemical processes occurring at the AA7075-T7351/1.0 M HCl interface was studied using EIS. Figure 9 shows the Nyquist plots for AA7075-T7351 in the presence and absence of the studied inhibitor. It can be seen that the capacitive loops' impedance spectroscopy signals in the presence of TA were generated as a result of the deposition of TA on the AA7075-T7351/solution interface. The inference being that AA7075-T7351 corrosion inhibition was as a result of direct surface coverage mechanism [43, 44], due to the adsorption of TA molecules. Also increasing the concentration of TA in 1 M HCl did not distort the capacitive loop of the Nyquist plot, indicating that the mechanism of adsorption of TA on AA7075-T7351 did not change. Figure 10 shows the simple electrochemical circuit used in analysing the electrochemical impedance data, consisting of solution resistance, (R_s), charge transfer resistance, (R_{ct}), inductive resistance, (R_L) and constant phase element, (CPE). The mathematical description of CPE impedance, takes a similar form as that of a capacitor, the only difference being that its phase angle no longer depends on frequency:

$$Z_{\text{CPE}} = \frac{1}{Q_o(j\omega)^n} \quad (13)$$

where Q_o is the CPE with a numerical value of admittance, n is an exponent ranging from -1 (in this case $1/Q_o$ is equal to inductance), 0 (Q_o equals admittance and there is low surface inhomogeneity), 0.5 (Z_{CPE} equals the Warburg impedance) and 1 (Q_o equals to capacitance), j is an imaginary number.

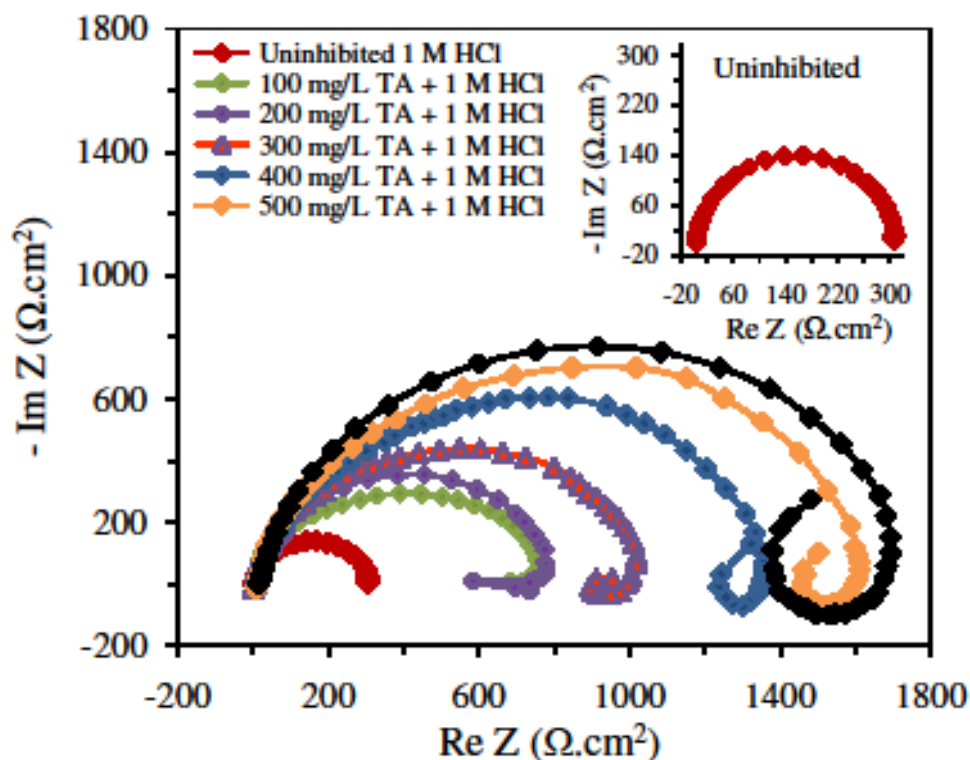


Figure 9: Nyquist plots for AA7075-T7351 in 1.0 M HCl in the absence and presence of TA

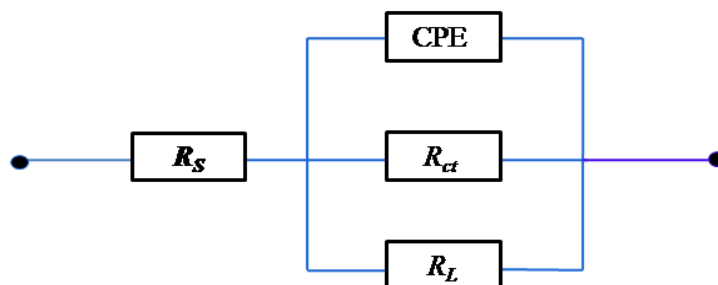


Figure 10: Equivalent circuit used in fitting the electrochemical impedance spectra

Table 4 shows the EIS parameters obtained after fitting the EIS spectra. The n values for the presence of TA are higher than that in the absence of TA, indicating a higher surface smoothness/homogeneity with more TA. This is attributed to the formation of a protective layer on the AA7075-T7351 surface. This is corroborated by the bode plots shown in figure 11, which showed increased phase angle as the concentration of TA increased. However, at the intermediate portions of the bode plots, table 5 shows increased values of the slopes of the linear region, indicating the existence of a protective layer on the AA7075-T7351 surface. Moreover, the values of the exponent are approximately equal to one, implying that the AA7075-T7351/electrolyte interface behaved like a pseudo capacitor. The double layer capacitance was calculated using;

$$C_{dl} = \frac{1}{2\pi f_{max} \left(\frac{R_{ct}R_L}{R_{ct}+R_L} \right)} \quad (14)$$

where f_{max} is the frequency corresponding to the maximum imaginary impedance.

Table 4: EIS parameters for AA7075-T7351 in 1.0 M HCl in the absence and presence of different concentrations of TA

System (in 1.0 M HCl)	R_s ($\Omega \cdot \text{cm}^2$)	R_L ($\Omega \cdot \text{cm}^2$)	R_{ct} ($\Omega \cdot \text{cm}^2$)	n	C_{dl} ($\mu\text{F} \cdot \text{cm}^{-2}$)	Surface coverage (θ)	IE %
Uninhibited	1.93	5.18	309.8	0.892	32.40		
100 mg/L TA	2.44	47.47	795.9	0.910	15.89	0.61	61.1
200 mg/L TA	1.91	153.06	817.5	0.921	12.29	0.62	62.1
300 mg/L TA	2.21	195.44	1046.1	0.928	10.61	0.70	70.4
400 mg/L TA	3.31	207.62	1367.2	0.929	6.06	0.77	77.3
500 mg/L TA	3.70	216.91	1643.6	0.933	3.96	0.81	81.2
1000 mg/L TA	5.58	1319.4	1745.1	0.942	2.16	0.82	82.3

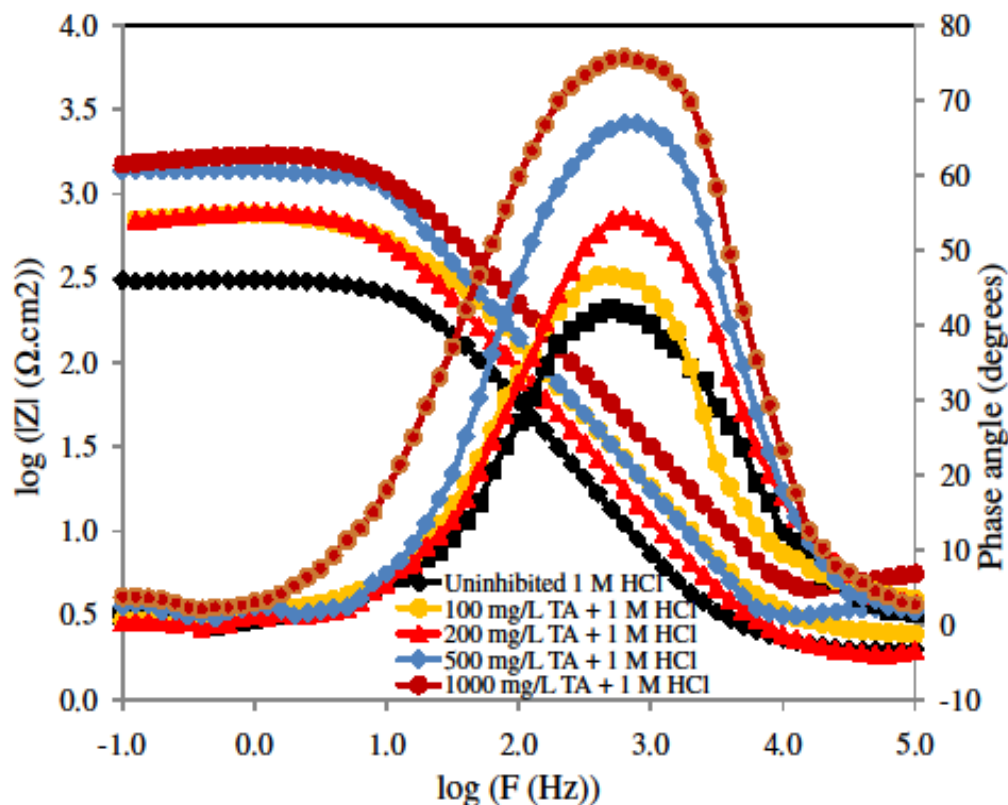
**Figure 11:** Bode plots for AA7075-T7351 in 1.0 M HCl in the absence and presence of TA

Table 4 shows that R_s , R_L and R_{ct} increased with increased TA concentrations. This was so because when the frequency was equal to zero, Z_{CPE} became infinite (blocked current flow), the inductive impedance reduced to the ohmic part (since there is no such thing as an ideal inductor), R_L , then coupled with the charge transfer resistance, R_{ct} , to limit current flow and by extension improved the inhibition efficiency. The increases in resistances were as a result of double layer formation by the TA molecules.

Table 5: Values of slopes, intercepts, correlation coefficients and phase angles obtained from the Bode plots of AA7075-T7351 in 1.0 M HCl in the absence and presence of different concentrations of TA

System (1.0 M HCl)	Slope ($\log \Omega$ /decade)	Intercept K Ω	R^2	Phase Angle
Uninhibited	-0.678	1.24	-0.989	42.2°
100 mg/L TA	-0.817	5.20	-0.997	46.6°
200 mg/L TA	0.822	3.60	-0.995	54.5
500 mg/L TA	-0.874	7.52	-0.997	66.9
1000 mg/L TA	-0.851	9.14	-0.998	75.7

Conclusion

The outcome of the experimental study in the use of *Treculia africana*(TA) leaf extracts as corrosion inhibitor for AA7075-T7351 in 1.0 M HCl solution showed that it effectively inhibited corrosion at room temperature conditions by forming an AA7075-T7351 - TA complex, which behaved like a barrier hindering further attack of the metal. However, these barrier weakened at elevated temperatures. TA leaves extract acts like a mixed type inhibitor whose efficiency increases with increases in concentration. The TA leaves extracts on the AA7075-T7351 surface obey the Langmuir, Freundlich and Temkin adsorption isotherm, in that order, by way of physisorption and chemisorption mechanisms. The gravimetric, electrochemical impedance spectroscopy and potentiodynamic polarization results are in good agreement with each other and affirm TA as a mixed-type inhibitor. Increasing negative values of Bode slopes, which are approximately equal to negative of unity, was further proof that TA formed protective layers on AA7075-T7351.

References

1. J. Hemanth, Quartz (SiO₂p) reinforced chilled metal matrix composite (CMMC) for automotive applications, *Materials and Design*, 30 (2) (2009) 323 - 329
2. M. T. Sijo and K. R. Jayadevan Analysis of stir cast aluminium silicon carbide metal matrix composite: A comprehensive review, International conference on Emerging Trends in Engineering, Science and Technology, *Procedia Technology*, 24 (2016) 379 - 385
3. A. Baradeswaran and P. A. Elaya, Study on mechanical and wear properties of 7075/Al₂O₃/graphite hybrid composites, *Composites: Part B*, 56 (2014) 464 - 471.
4. I. Radojčić, K. Berković, S. Kovac, and J. Vorkapić- Furac, Natural honey and black radish juice as tin corrosion inhibitors, *Corrosion Science*, 50 (2008) 1498 - 1504.
5. F. Andreatta, H. Terryn, J. H. W. de Wit, Corrosion behaviour of different tempers of AA7075 aluminium alloy, *Electrochimica Acta*, 49 (17 - 18) (2003) 2851 - 2862, <https://doi.org/10.1016/j.electacta.2004.01.046>
6. D. E. J. Talbot and J. D. R. Talbot, *Corrosion Science and Technology*. Boca Raton: CRC press, Florida, (2018) p23.
7. X. Zheng, M. Gong, Q. Li, and L. Guo, Corrosion inhibition of mild steel in sulfuric acid solution by loquat (*Eriobotrya japonica* Lindl.) leaves extract, *Scientific Reports*, 8 (2016) 9140, DOI:10.1038/s41598-018-27257-9.
8. P. Muthukrishnan, P. Prakash, B. Jeyaprabha, and K. Shankar, Stigmasterol extract from *Ficushispida* leaves as a green inhibitor for the mild steel corrosion in 1 M HCl solution, *Arabian Journal of Chemistry*, (2015), <http://dx.doi.org/10.1016/j.arabjc.2015.09.005>
9. D. R. Arnott, B. R. W. Hinton and N. E. Ryan, Cationic- film-forming inhibitors for the protection of the AA7075 aluminium alloy against corrosion in aqueous chloride solution. *Corrosion*, 45 (1) (1989) 12 - 18
10. D. A. Winkler, M. Breedon, A. E. Hughes, F. R. Burden, A. S. Barnard, T. G. Harvey and I. cole, Towards chromate-free corrosion inhibitors: structure-property models for organic alternatives. *Green Chemistry*, 16 (6) (2014) 3349 - 3357
11. T.G. Harvey, S.G. Hardin, A.E. Hughes, T.H. Muster, P.A. Corrigan, J. Mardel, S.J. Garcia, J.M.C. Mol, A.M. Glenn, The effect of inhibitor structure on the corrosion of AA2024 and AA7075, *Corrosion science*, 53 (6) (2011) 2184 - 2190
12. K. R. Ansari, M. A. Quraishi, and A. Singh, Isatin derivatives as a non-toxic corrosion inhibitor for mild steel in 20% H₂SO₄, *Corrosion Science*, 95 (2015) 62 - 70
13. V.S. Saji, A review on recent patent in corrosion inhibitors, *Recent Patents on Corrosion Science*, 2 (2010) 6-12
14. C. Verma, M. A. Quraishi, E. E. Ebenso, I. B. Obot, and A. El Assyry, 3-Amino alkylated indoles as corrosion inhibitors for mild steel in 1 M HCl: Experimental and theoretical studies, *Journal of Molecular Liquids*, 219 (2016) 647 - 660
15. Y. C. Sharma and S. Sharma, Corrosion of Aluminum by *Psidium Guajava* Seeds in HCl Solution, *Portugaliae Electrochimica Acta*, 34 (6) (2016) 365 - 382
16. L. A. Nnanna, K. O. Uchendu, G. Ikwuagwu, W. O. John, and U. Ihekoronye, Inhibition of Corrosion of Aluminum Alloy AA8011 in Alkaline Medium Using *Palisota hirsute* Extract, *International Letters of Chemistry, Physics and Astronomy*, 67 (2016) 14 - 20

17. L. Chafki, E. H. Rifi, R. Touri, M. E. Touhami, and Z. Hatim, Corrosion Inhibition Mild Steel in 1.0 M HCl Solution by Anhydrous Tricalcium Phosphate, *The Open Materials Science Journal*, 12 (2018) 69
18. M. Goyal, S. Kumar, I. Bahadur, C. Verma, and E. E. Ebenso, Organic corrosion inhibitors for industrial cleaning of ferrous and non-ferrous metals in acidic solutions: review. *A review Journal of Molecular Liquids*, 256 (2018) 563 - 57
19. A. A. Nazeer, M. Madkour, Potential use of smart coatings for corrosion protection of metals and alloys: A review, *Journal of Molecular Liquids*, 253 (2018) 11 – 22
- 20 N. Chaubey, V. K. Singh, and M. A. Quraishi, Electrochemical approach of *Kalmegh* leaf extract on the corrosion behavior of aluminium alloy in alkaline solution. *International Journal of Industrial Chemistry*, 8 (2017) 75 – 82
- 21 C. C. Okoro, O. Samuel and J. Lin, The effects of Tetrakis-hydroxymethyl phosphonium sulfate (THPS), nitrite and sodium chloride on methanogenesis and corrosion rates by methanogen populations of corroded pipelines. *Corrosion Science*, 112 (2016) 507 – 516
- 22 H. Pratikno and H. S. Titah Bio-corrosion on Aluminium 6063 by *Escherichia coli*, in Marine Environment. *IPTEK, The Journal for Technology and Science*, 28 (2) (2017) 55 - 58
- 23 N. Raghavendra, and J. I. Bhat, Natural Products for Material Protection: An Interesting and Efficacious Anticorrosive Property of Dry Arecanut Seed Extract at Electrode (Aluminum)–Electrolyte (Hydrochloric Acid) Interface. *J. Bio. Tribo. Corros.*, 2 (2016) 21
- 24 A. Ennouri, A. Lamiri, and M. Essahli, Corrosion Inhibition of Aluminium in Acidic Media by Different Extracts of *Trigonella foenum-graecum* L Seeds *Portugaliae Electrochimica Acta*, 35 (5) (2017) 279 - 295
- 25 B. A. Abd-El-Naby, O. A. Abdullatef, H. M. El-Kshlan, E. Khamis, and M. A. Abd-El-Fatah, Effect of Alkaline Etching on the Inhibition of the Acidic Corrosion of Aluminum by Lupine Extract. *Portugaliae Electrochimica Acta* 33(1) (2015) 1 - 11
- 26 E. E. Oguzie, Corrosion inhibition of aluminium in acidic and alkaline media by *Sansevieria trifasciata* extract. *Corrosion Science*, 49 (2007) 1527 – 1539
- 27 N. Chaubey, D.K. Yadav, V.K. Singh, M.A. Quraishi, A comparative study of Extracts for corrosion inhibition effect on aluminium alloy in alkaline medium. *Ain Shams Engineering Journal*, 8(4) (2017) 673 - 682
- 28 N. Chaubey, V. K. Singh, and M. A. Quraishi, Effect of some peel extracts on the corrosion behavior of aluminum alloy in alkaline medium, *International Journal of Industrial Chemistry*, 6 (2015) 317 – 328
- 29 A. H. Al-Moubaraki, A. A. Al-Howiti, M. M. Al-Dailami, and E. A. Al-Ghamdi, Role of aqueous extract of celery (*Apium graveolens* L.) seeds against the corrosion of aluminium/sodium hydroxide systems. *Journal of environmental chemical engineering* 5(5) (2017) 4194 - 4205
30. P. M. Ejikeme, S. G. Umana and O. D. Onukwuli, Corrosion Inhibition of Aluminium by *Treculia Africana* Leaves Extract in Acid Medium, *Portugaliae Electrochimica Acta*, 30 (5) (2012) 317 - 328, <https://doi:10.4152/pea.201205317>
31. B. J. Harbone, *Phytochemical Methods-A Guide to Modern Techniques of Plant Analysis*, London: *Chapman and Hall*; 1998.
32. Standard practice for preparing, cleaning, and evaluating corrosion test specimens, *ASTM G1 - 03 2003* standard.
33. L. A. Nnanna, O. C. Nwadiuko, N. D. Ekekwe, C. F. Ukpabi, S. C. Udensi, K. B. Okeoma, B. N. Onwuagba, I. M. Mejeha, Adsorption and Inhibitive Properties of Leaf Extract of *Newbouldia leavis* as a Green Inhibitor for Aluminium Alloy in H₂SO₄, *American Journal of Materials Science*, 2011; 1 (2) 143 - 148, [DOI:10.5923/j.materials.20110102.24](https://doi.org/10.5923/j.materials.20110102.24)
34. Standard practice for Laboratory immersion corrosion testing of metals, *ASTM G31 - 72* (re-approved 2004).
35. C. Verma, L. O. Olasunkanmi, E. E. Ebenso, M. A. Quraishi, and I. B. Obot, Adsorption Behavior of Glucosamine-Based, Pyrimidine-Fused Heterocycles as Green Corrosion Inhibitors for Mild Steel: Experimental and Theoretical Studies. *J. Phys. Chem. C*, 120 (2016) 11598 – 11611
36. P. Muthukrishnan, B. Jeyaprabha, and P. Prakash, Adsorption and corrosion inhibiting behaviour of *Lannea coromandelica* leaf extract on mild steel corrosion, *Arabian Journal of Chemistry*, 10 (2017) S2343 – S2354
37. N. B. Iroha and L. A. Nnanna, Electrochemical and Adsorption Study of the anticorrosion behavior of Cefepime on Pipeline steel surface in acidic Solution, *J. Mater. Environ. Sci.*, 10 (10) (2019) 898 - 908
38. C. Verma, L.O. Olasunkanmi, E.E. Ebenso, M.A. Quraishi, Adsorption characteristics of green 5-aryl amino methylene pyrimidine-2,4,6-triones on mild steel surface in acidic medium: Experimental and computational approach, *Results in Physics*, 8 (2018) 657–670
39. S. Manimegalai and P. Manjula, Thermodynamic and Adsorption studies for corrosion Inhibition of Mild steel in Aqueous Media by *Sargassum swartzii* (Brown algae), *J. Mater. Environ. Sci.*, 6 (6) (2015) 1629 - 1637

40. Soltani, N., Tavakkoli, N., Kashani, M.K., Mosavizadeh, A., Oguzie, E.E., Jalali, M.R., *Silybum marianum* extract as a natural source inhibitor for 304 stainless steel corrosion in 1.0 M HCl, *J. Ind. Eng. Chem.*, 20 (2013) 3217 – 3227
41. L. A. Nnanna, Electrochemical study of corrosion inhibition of mild steel in acidic solution using *Gnetum Africana* leaves extracts. *British Journal of Applied Sciences & Technology*, 5(6) (2015) 556 - 567
42. R. Solmaz, Investigation of corrosion inhibition mechanism and stability of Vitamin B1 on mild steel in 0.5M HCl solution. *Corrosion Science*, 81 (2014) 75 – 84
43. Y. Elkhotfi, I. Forsal, E .M. Rakib and B. Mernari, The Inhibition Action of Essential Oil of J. *Juniperus Phoenicea* on the Corrosion of of Mild Steel in Acidic Media, *Portugaliae Electrochimica Acta*, 36 (2) (2018) 77-87
44. N. K. Gupta, M. A. Quraishi, P. Singh, V. Srivastava, K. Srivastava, C. Verma and A. K. Mukherjee, *Curcumine Longa*: Green and Sustainable Corrosion Inhibitor for Aluminium in HCl Medium, *Analytical and Bioanalytical Electrochemistry*, 9 (2) (2017) 245 - 265
45. S.S. Shivakumar, and K.N. Mohana, Studies on the Inhibitive Performance of *Cinnamomum zeylanicum* Extracts on the Corrosion of Mild Steel in Hydrochloric Acid and Sulphuric Acid Media, *J. Mater. Environ. Sci.* 4 (3) (2013) 448-459
46. K. H. Hassan, A. A. Khadom and N. H. Kurshed, Citrus aurantium leaves extracts as a sustainable corrosion inhibitor of mild steel in sulfuric acid, *South African Journal Of Chemical Engineering* 22 (2016) 1 - 5
47. E. Ituen, O. Akaranta and A. James, Evaluation of Performance of Corrosion Inhibitors Using Adsorption Isotherm Models: An Overview, *Chemical Science International Journal*, 18 (1) (2017) 1-34

(2019) ; <http://www.jmaterenvirosci.com>